Transp Porous Med
DOI 10.1007/s11242-014-0275-x

Nonlinear Inversion of an Unconfined Aquifer: Simultaneous Estimation of Heterogeneous Hydraulic Conductivities, Recharge Rates, and Boundary Conditions

Ye Zhang

Received: 23 May 2013 / Accepted: 7 January 2014

Abstract A new inverse method is developed to simultaneously estimate heterogeneous hydraulic conductivities, source/sink rates, and unknown boundary conditions for steady-state flow in an unconfined aquifer. Unlike objective function-based techniques, the new method does not optimize any data-model misfits. Instead, its formulation is developed by honoring physical flow principles as well as observation data at sampled locations. Under the Dupuit–Forchheimer assumption of negligible vertical flow, accuracy and stability of the new method are demonstrated using synthetic heterogeneous aquifer problems with increasingly complex flow: (1) aquifer domains without source/sink effects; (2) aquifer domains with a point sink (a pumping well operating under a constant discharge rate); (3) aquifer domains with constant or spatially variable recharge; (4) aquifer domains with constant or spatially variable recharge undergoing single-well pumping. For all problems, inversion yields stable solutions under increasing head measurement errors (up to ± 10 % of the total head variation in a problem), although accuracy of the estimated parameters degrades with the increasing errors. The inverse method is successfully tested on problems with high hydraulic conductivity contrasts—up to 10,000 times between the maximum and minimum values. In inverting several heterogeneous problems, if the aquifer is assumed homogeneous with a constant recharge rate, physically meaningful parameter estimates (i.e., equivalent conductivities and mean recharge rates) can be determined. Alternatively, if the inverse parameterization contains spurious parameters, inversion can identify such parameters, while the simultaneous estimation of non-spurious parameters is not affected. The method obviates the well-known issues associated with model "structure errors", when inverse parameterization either simplifies or complexifies the true parameter field.

Keywords Unconfined aquifer · Inversion · Hydraulic conductivity · Recharge rate · Boundary conditions

Y. Zhang (✉)
University of Wyoming, 1000 University Ave., Laramie, WY, USA
e-mail: yzhang9@uwyo.edu

Published online: 02 February 2014

1 Introduction

Unconfined aquifers, or water table aquifers, underlie most areas of the earth and are important freshwater resources. Water table variation of unconfined aquifers is subject to direct infiltration of rainfall recharge, or losses due to evapotranspiration, while pumping (and less frequently, injection) modifies the water table locally near wells. In unconfined aquifers, groundwater flow is not only influenced by the intrinsic hydraulic parameters of the aquifer, e.g., hydraulic conductivity (K), transmissibility (T), storage coefficients, but also the source/sink effects as a result of recharge, evapotranspiration, and well operations. For scientific and management purposes, there exists a need to estimate not only the hydraulic parameters of an unconfined aquifer, but also the parameters characterizing its source/sink strengths. For an unconfined aquifer, this study focuses on the simultaneous estimation of hydraulic conductivities, recharge rates, and the unknown (steady-state) aquifer boundary conditions, based on observation data such as hydraulic heads, groundwater fluxes, or pumping rates.

A variety of techniques exist for estimating conductivities and recharge rates for unconfined aquifers. Traditional aquifer test methods develop analytical solutions or type curves based on the assumption that aquifer conductivity is homogeneous (Dagan 1967; Neuman 1972), or aquifer exhibits simple layering (Hantush and Jacob 1955), although conductivity estimated with such assumptions may exhibit "scale effect" due to aquifer heterogeneity (Neuman 1994; Sanchez-Vila et al. 1996; Schulze-Makuch et al. 1999). Other techniques, including slug tests, borehole flowmeters, and geophysical measurements, can estimate conductivities of small aquifer volumes near wellbores (Cooper et al. 1967; Bouwer and Rice 1976; Dagan 1978; Zlotnik and Zurbuchen 2003; Darnet et al. 2003; Crisman et al. 2007). Methods have also been developed that combine geostatistics with the inverse theory to directly infer heterogeneous aquifer conductivity, while quantifying its estimation uncertainty (Li et al. 2008; Liu et al. 2008; Cardiff et al. 2009). In many studies, source/sink effects are either not accounted for, assumed known, or eliminated using specialized formulations. As a result, conductivity estimation tends to be the focus of the investigations, while recharge (or evapotranspiration) rate is rarely estimated. Moreover, many techniques exist for estimating the recharge rate (N) of an unconfined aquifer (Simmers 1998): some are based on water or chemical mass balances (Dettinger 1989; Scalon et al. 2002; Healy and Cook 2002; Tan et al. 2007; Lin et al. 2009), others infer recharge rates from physically-based, highly detailed, vadose-zone or rainfall-runoff models (Pan et al. 1997; Russo et al. 2001; Jyrkama et al. 2002), while still others use model calibration to infer the recharge rate(s) as one or more unknown model parameters (Portniaguine and Solomon 1998; Moench et al. 2001; Hill and Tiedeman 2007). With the exception of model calibration, with which aquifer conductivity and recharge rate can be simultaneously estimated, many methods assume conductivity to be known, homogeneous, or piecewise homogeneous.

In natural systems, both aquifer conductivity and aquifer recharge rate are typically variable in space. To simultaneously estimate these parameters, inverse techniques offer the most flexibility. On the one hand, if large amounts of aquifer characterization data are collected, these techniques can act as a data integration tool to help develop highly detailed flow models (McKenna and Poeter 1995; Harvey and Gorelick 1995; Day-Lewis et al. 2006; Reynolds and Marimuthu 2007; Fienen et al. 2009; Sakaki et al. 2009; Keating et al. 2010; Liu and Kitanidis 2011). On the other hand, in data-poor environments, such techniques can help develop insights into the types of observation data to collect that are important for estimating different parameters (Carrera and Neuman 1986; Tiedeman et al. 2003; Saiers et al. 2004; Hill and Tiedeman 2007). However, most of the existing inverse methods are developed by minimizing an objective function, which is typically defined as a form of mismatch between

measurement data and the corresponding model simulated values (Hill and Tiedeman 2007; Oliver et al. 2008). During inversion, parameters are updated iteratively using a forward model that provides the link between the parameters and the data. Because a forward model is needed, boundary conditions (BC) of the model are either assumed known, or are calibrated as part of the inversion process. However, objective function-based techniques may lead to non-uniqueness in the estimated parameters and model BC, even for relatively simple problems. To address this issue, a new steady-state aquifer inverse theory was developed, adopting a set of approximating functions of hydraulic head and groundwater fluxes as the fundamental solutions of inversion (Irsa and Zhang 2012). By enforcing the continuity of these functions at a set of collocation points on the interfaces of the inversion grid cells, physics of flow was preserved locally within each cell and globally extending to the boundary. To incorporate noisy observed data, the method penalized the mismatch between the measurements and the values predicted by the fundamental solutions. After enforcing the continuity constraint and the data fit requirement, inversion led to a system of linear equations that can be solved with least-squares techniques. Parameters were estimated from the solution of these equations, based on which heads and flow fields were reconstructed directly from the approximating functions. Boundary conditions were then inferred from these fields.

The method described in Irsa and Zhang (2012), however, has limitations. First of all, the governing flow equation must be linear for which the approximating functions can be obtained via integration, which leads to a set of polynomial functions. This limits the applicability of the method to confined aquifer problems without source/sink effects. Second, because source/sink effects (e.g., pumping well) cannot be accommodated, groundwater flux or flow rate measurements must be sampled from the subsurface. In theory, such measurements can be obtained using borehole logging or baseflow separation techniques, but both the cost and the level of measurement uncertainty are expected to be high. Third, for problems with multiple hydrofacies, only a single hydrofacies conductivity can be estimated: conductivities of the other hydrofacies are estimated using known ratios that are specified as a set of prior information equations. For unconfined aquifers for which the flow equation is nonlinear and source/sink effects are important, the method proposed by Irsa and Zhang (2012) is not applicable. This study improves the previous work by developing a new unconfined aquifer inverse method, where the aquifer is subject to areal recharge, well discharge, or both. Multiple can be hydraulic conductivities (Ks), recharge rates (Ns), as well as the unknown model BC can be simultaneously estimated, i.e., known ratios between parameters are no longer needed. The unconfined flow equation is linearized, allowing its solution by analytical techniques. Specifically, depending on the type of aquifer forcing, the fundamental solutions of inversion are obtained by superposing appropriate analytical flow solutions for homogeneous sub-domains. Compared to those developed in Irsa and Zhang (2012), these solutions are considered physically-based. Due to linearization and superposition, inversion gives rise to a system of nonlinear equations, for which nonlinear equation solvers are used.

To condition the inverse method, observation data include hydraulic heads and a minimum of one measurement related to its gradient, e.g., Darcy flux or flow rate. Flux or flow rate data are needed because unconfined aquifer parameter estimation suffers a well-known issue of parameter identifiability. For example, if a homogeneous unconfined aquifer is receiving uniform recharge, the flow equation is: $\nabla^2 h^2 = -2N/K$, where ∇^2 is the Laplace operator. Clearly, as long as the ratio of recharge versus conductivity remains the same, infinite combinations of these two parameters can yield identical hydraulic head distribution in the aquifer. *Fitting or inverting only the hydraulic head data, therefore, cannot lead to unique and simultaneous estimation of both parameters*. Measurements related to the hydraulic head gradient must be provided, and this limitation cannot be overcome with any inverse methods.

However, in view of the difficulty in subsurface sampling, for aquifers with nonuniform distributions of K and N, we investigate problems whereby a single pumping rate, in addition to head measurements, is provided to inversion. Because well rates can be easily measured at the surface, data requirement for this problem is not much greater than that needed for interpreting pumping tests. Clearly, the method would be less useful if individual hydrofacies heterogeneity required a separate well rate (i.e., head gradient) measurement.

Moreover, with traditional inversion techniques, if small-scale parameter heterogeneities are ignored during inversion, model "structure errors" can arise that conuld lead to biased parameter estimates (Cooley and Christensen 2005; Gaganis and Smith 2008; Doherty and Welter 2010). In this work, the jointly estimated Ks and Ns will be tested for biases. For example, at sites where detailed measurements are not available, the inverse method should provide physically meaningful bulk parameter estimates that represent the effect of underlying parameter variations on flow. On the other hand, due to incomplete understanding of the flow process, spurious parameters can be introduced into inversion. Several problems are tested by developing inverse parameterizations that (1) do not explicitly account for small-scale heterogeneities ("simplifying" model structure error), and (2) contain spurious parameters ("complexifying" model structure error). For (1), the inverse solution is considered unbiased if an equivalent conductivity and average recharge rate can be simultaneously estimated along with the unknown model BC. For (2), an unbiased solution is defined as one where the inverse solution reveals the existence of spurious parameters, while the simultaneous estimation of non-spurious parameters is not affected.

To test the accuracy of the new method, a suite of one-dimensional (1D) inversions is conducted for synthetic heterogeneous aquifers with increasingly complex flow: (1) aquifer domains without source/sink effects; (2) aquifer domains with a point sink (a pumping well operating under a constant discharge rate); (3) aquifer domains with constant or spatially variable recharge rates; (4) aquifer domains with constant or spatially variable recharge rates undergoing single-well pumping. All test problems employ a hydrofacies parameterization in the distributions of conductivity and recharge rate, data requirement is thus low, e.g., up to 20 observed hydraulic heads and a few flux or flow rate measurements are used to condition the inversion. For problems (2) and (4), only a single pumping rate (in addition to hydraulic heads) are provided. For select problems, stability of inversion is investigated by adding increasingly larger measurement noise to the observed heads. The inverse solution is considered stable if small measurement errors do not lead to large estimation errors. In the remainder of this article, the inverse theory is introduced first, followed by results testing the above set of problems, whereby the inverse solution is compared to the "true" solution of a forward model. Issues related to stability, accuracy, and structure errors are addressed. Limitations and future research are indicated, before results are summarized in the Conclusion section.

2 Theory

2.1 The Forward Problem

Under the Dupuit–Forchheimer assumption of negligible vertical flow, steady-state groundwater flow equation in an unconfined aquifer with a horizontal base is:

$$\frac{\partial}{\partial x}\left(Kh\frac{\partial h}{\partial x}\right)+\frac{\partial}{\partial y}\left(Kh\frac{\partial h}{\partial y}\right)+N(x,y)=Q_{\mathrm{w}}\delta\left(\mathbf{x}-\mathbf{x}_0\right)\quad\text{in}\quad\Omega \tag{1}$$

where Ω is the solution domain, $\mathbf{x} = (x; y)$ is horizontal coordinate, h is hydraulic head (the horizontal aquifer base is set as head datum), K is depth-averaged, locally isotropic hydraulic conductivity, $N(x, y)$ is areal source/sink (only recharge is evaluated in this work), Q_{w} is pumping rate at $\mathbf{x}_0$, and δ represents a Dirac delta function. Equation (1) is nonlinear, but will be linearized in developing the inverse solution.

Given a set of boundary conditions, hydraulic conductivities, and recharge rates, Eq. (1) can be solved with a forward model, which is used in this work to provide a set of observation data for the inverse analysis. In solving the forward model, besides no-flow boundaries, Dirichlet boundary condition is assigned:

$$h = g(x, y) \quad \text{on} \quad \Gamma \tag{2}$$

where Γ is the Dirichlet-type model boundary and $g(x, y)$ describes a set of specified heads on Γ.

2.2 The Inverse Problem

In formulating the inverse solution, two sets of constraint equations are enforced, following Irsa and Zhang (2012): (1) global continuity of hydraulic head and Darcy flux throughout Ω; (2) local conditioning of head, flux, and/or flow rate by measurements. With these constraints, the inverse system of equations becomes well-posed when sufficient measurement data are provided, leading to fast and stable solution (detail is provided later). The constraint equations imposing the head and flux continuities are written as:

$$\begin{aligned} &\int \delta(p_l - \varepsilon) R_{\mathrm{h}}(\zeta_i) d\zeta_i = 0 \\ &\int \delta(p_l - \varepsilon) R_{\mathrm{q}}(\zeta_i) d\zeta_i = 0 \\ &i = 1, \ldots, m; \\ &l = 1, \ldots, n \end{aligned} \tag{3}$$

where $R_{\mathrm{h}}(\zeta_i)$ and $R_{\mathrm{q}}(\zeta_i)$ are a set of residual equations of the hydraulic head and Darcy flux, respectively, written at the ith cell interface (ζ_i) of the inverse grid (a grid used for solving the inverse problem), m is the total number of interfaces, p_l is a collocation point on the interface, n is the number of collocation points per interface ($n = 1$ for 1D inversion). $\lim_{\varepsilon \to 0} \delta(p_l - \varepsilon) = 1$, $\delta(p_l - \varepsilon)$ is a Dirac delta weighting function. The continuity constraints are, therefore, enforced at the collocation points on the interfaces. In Irsa and Zhang (2012), $\delta(p_l - \varepsilon)$ less than 1.0 was used, as this tended to stabilize or accelerate the linear equation solver. In this work, $\delta(p_l - \varepsilon)$ is not found to play a role in the speed of the convergence of the nonlinear solvers. It is assigned a value of 1.0 and the continuity constraint is strongly enforced.

Both residual equations can be expanded as:

$$\begin{aligned} R_{\mathrm{h}}(\zeta_i) &= \widetilde{h}^j(\zeta_i) - \widetilde{h}^k(\zeta_i) \\ R_{\mathrm{q}}(\zeta_i) &= \widetilde{q}^j(\zeta_i) - \widetilde{q}^k(\zeta_i) \end{aligned} \tag{4}$$

where $\widetilde{h}$ and $\widetilde{q}$ are the proposed fundamental solutions of inversion; j and k denote grid cells adjacent to each interface. In Irsa and Zhang (2012), flow in a confined aquifer without source/sink was described by the Laplace equation. $\widetilde{h}$ was, therefore, proposed as the real part of any complex holomorphic function. Because no source/sink existed, flow field was uniform for which a mathematical solution of the Laplace equation was a polynomial function.

A quadratic function was adopted in Irsa and Zhang (2012) to approximate the head, which allowed its 1^{st} order differentiation to obtain linear flux functions (alternatively, higher order polynomials can be adopted, which can ensure continuity of the flux derivatives. Accordingly, Eq. (4) needs to be expanded to include additional continuities). For unconfined aquifers, to address the nonlinearity of the flow equation, a new set of fundamental solutions will be developed (see Sect. 2.3).

The constraint equations imposing penalties on data misfits can be written as:

$$\begin{gathered}\delta(p_t-\varepsilon)\left(\widetilde{h}(p_t)-h^{\mathrm{o}}\right)=0\\ \delta(p_t-\varepsilon)\left(\widetilde{q}(p_t)-q^{\mathrm{o}}\right)=0\\ \delta(p_t-\varepsilon)\left(\widetilde{Q}(p_t)-Q^{\mathrm{o}}\right)=0\\ t=1,\ldots,T\end{gathered} \tag{5}$$

where p_t is a measurement location at which h^{o}, q^{o}, or Q^{o} are sampled, T is the total number of measurements. In the last equation of Eq. (5), p_t is any contour or surface along which $\widetilde{Q}$ can be integrated from the flux approximating functions. $\delta(p_t-\varepsilon)$ is a weighting function assigned to each equation to reflect the magnitude of the measurement errors. If error-free measurements are used, $\delta(p_t-\varepsilon)=1.0$. Moreover, as will be demonstrated later, as few as a single well rate, in addition to hydraulic heads, suffices to provide the necessary measurement for the inversion to succeed. Therefore, not all equations of Eq. (5) are needed for inversion: either flux or flow rate measurements are needed, but not both.

2.3 Fundamental Solutions

Prior to inversion, approximating functions of hydraulic head, Darcy flux, and flow rate are obtained from solving the flow equation within individual hydrofacies in which the hydraulic conductivity and the recharge rate are homogeneous. For each hydrofacies, Eq. (1) is rewritten as:

$$\frac{\partial^2(h^2)}{\partial x^2}+\frac{\partial^2(h^2)}{\partial y^2}+\frac{2N}{K}=\frac{2Q_{\mathrm{w}}}{K}\delta(\mathbf{x}-\mathbf{x}_0)\qquad in\quad \Omega_i \tag{6}$$

where Ω_i represents a hydrofacies ($i=1,\ldots,L$), $\Omega=\Omega_1\bigcup\Omega_2\bigcup\cdots\Omega_L$, L is the number of hydrofacies. Equation (6) is linear with respect to $h^2(x,y)$. Unlike Irsa and Zhang (2012), where the proposed hydraulic head was a second order polynomial to describe a uniform flow field, unconfined flow dynamics with source/sink effects entail a different set of approximating functions. These functions are developed by writing analytical solutions of Eq. (6) under different flow stimulus, as explained in Sect. 2.4 for each test problem.

The overall steps for solving the inverse problem are illustrated in Fig. 1. For a given problem, the flow equation for a homogeneous sub-domain is first simplified from Eq. (6), which yields a set of hydraulic head and Darcy flux solutions. Inversion then proceeds by writing Eq. (3) at all inverse grid cell interfaces and Eq. (5) (or a subset of it) at the locations where measurements are taken. Hydrofacies zonation pattern is assumed known, therefore, in creating the inverse grid, cell interfaces fall at the zone interfaces. A system of nonlinear equations is assembled and solved with nonlinear optimization (see Sect. 2.5). Once a solution is found, i.e., the estimated parameters and a set of head and flux approximating functions, boundary heads can be determined by sampling the appropriate functions at the model boundaries. Similarly, flux (or flow rate) boundary conditions can be recovered by sampling (or integrating) the appropriate flux functions. In this work, the recovered BC are presented as hydraulic heads at the boundaries.

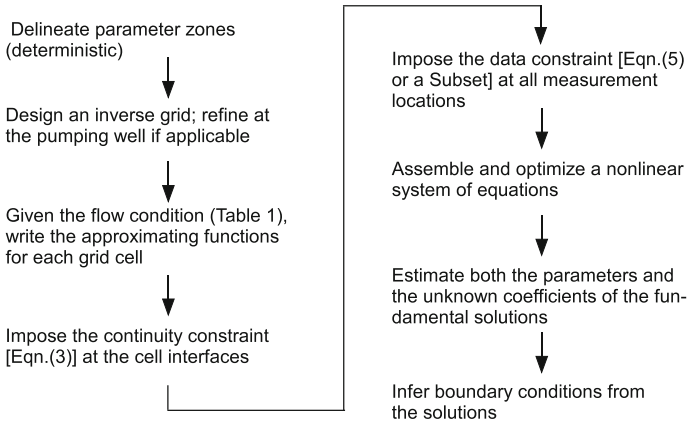

Fig. 1 Schematic diagram of the inverse method of this study

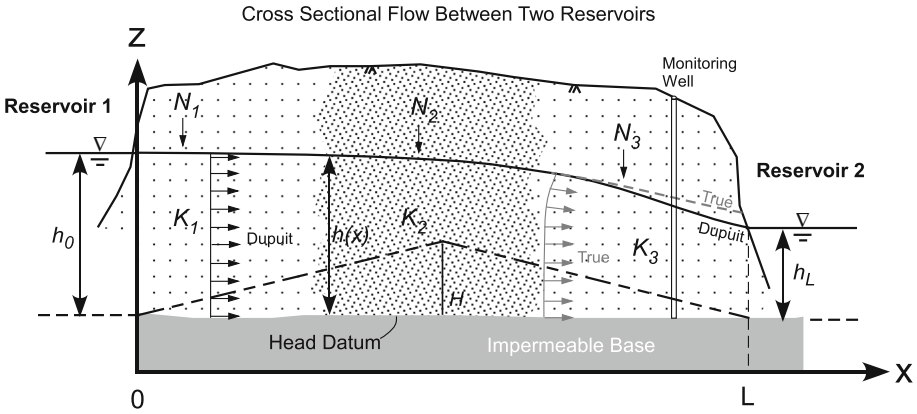

Fig. 2 Schematic diagram of steady-state flow in an unconfined aquifer between two reservoirs (modified after Bear 1972). Aquifer ranges from $x = 0$ to $x = L$. *Arrows* indicate the Darcy flux distribution under the Dupuit–Forchheimer assumption (*black*), or under the real condition (*gray*). A non-flat aquifer bottom is indicated by the *dashed line*, with a maximum height of H at $x = L/2$

2.4 Test Problems

The development of the fundamental solutions of inversion is illustrated with a set of test problems with increasingly complex flow. For each problem, a forward (true) model is first created to generate a set of observation data under a set of (true) model BC. Inverse analysis is then carried out according to the steps of Fig. 1. Inversion accuracy is evaluated by comparing the estimated parameters and the recovered BC against those of the forward model. For all test problems, aquifers overlie an impervious base, which is set as the head datum. The inverse solution is developed in one dimension that is aligned with the flow direction.

In test problem 1, the forward model describes flow between two constant head reservoirs where aquifer does not receive any recharge (Fig. 2). Under the Dupuit–Forchheimer assumption, vertical flow is ignored. The flow equation and the approximating functions for inversion are listed in Table 1. Clearly, $\widetilde{h}$ is the classic uniform flow solution with which $\widetilde{q}$ is

Table 1 Flow equations and the corresponding approximating functions for the test problems

Flow equation	$\widetilde{h}$	$\widetilde{q}$	Notes
Test problem 1: unconfined flow without source/sink			
$\frac{\partial^2(h^2)}{\partial x^2} + \frac{\partial^2(h^2)}{\partial y^2} = 0$	$\widetilde{h}^2(x) = a_0 + a_1 x$ [1]	$\widetilde{q}(x) = -\frac{Ka_1}{2\sqrt{a_0 + a_1 x}}$	Forward model is 2D for which a 1D analytical solution along the x axis can be found, i.e., flow along both y and z axes is ignored
Test problem 2: unconfined flow with a pumping well (no areal recharge)			
$\frac{1}{r}\frac{\partial}{\partial r}\left(r\frac{\partial h^2}{\partial r}\right) + \frac{1}{r^2}\frac{\partial^2 h^2}{\partial \theta^2} = \frac{2Q_w}{K}\delta(\mathbf{x} - \mathbf{x}_0)$	$\widetilde{h}^2(r) = a_0 + a_1 r + \frac{Q_w}{K\pi}\ln r$	$\widetilde{q}(r) = -\frac{Ka_1 + Q_w/\pi/r}{2\sqrt{a_0 + a_1 r + (Q_w/K/\pi)\ln r}}$	Forward model is 3D and is radially symmetric around the pumping well, where the origin of r is
Test problem 3: unconfined flow with areal recharge (no pumping)			
$\frac{\partial^2 h}{\partial x^2} + \frac{\partial^2 h}{\partial y^2} + \frac{N(x,y)}{T} = 0$	$\widetilde{h}(x) = -\frac{N}{2T}x^2 + a_0 x + a_1$	$\widetilde{q}(x) = \frac{Nx - Ta_0}{-\frac{N}{2T}x^2 + a_0 x + a_1}$	Forward model is 2D for which a 1D analytical solution along the x axis can be found, i.e., flow along both y and z axes is ignored
Test problem 4: unconfined flow with areal recharge and a pumping well			
$\frac{\partial^2(h^2)}{\partial x^2} + \frac{\partial^2(h^2)}{\partial y^2} + \frac{2N(x,y)}{K} = \frac{2Q_w}{K}\delta(\mathbf{x} - \mathbf{x}_0)$	$\widetilde{h}^2(r) = -\frac{N}{2K}r^2 + \frac{Q_w}{K\pi}\ln r + a_0$	$\widetilde{q}(r) = \frac{Nr - \frac{Q_w}{\pi r}}{2\sqrt{-\frac{N}{2K}r^2 + \frac{Q_w}{K\pi}\ln r + a_0}}$	Forward model is 3D and is radially symmetric around the pumping well, where the origin of r is

[1] a_0 and a_1 are the unknown coefficients defined for each inverse grid cell. The flow equations are simplified from Eq. (6)

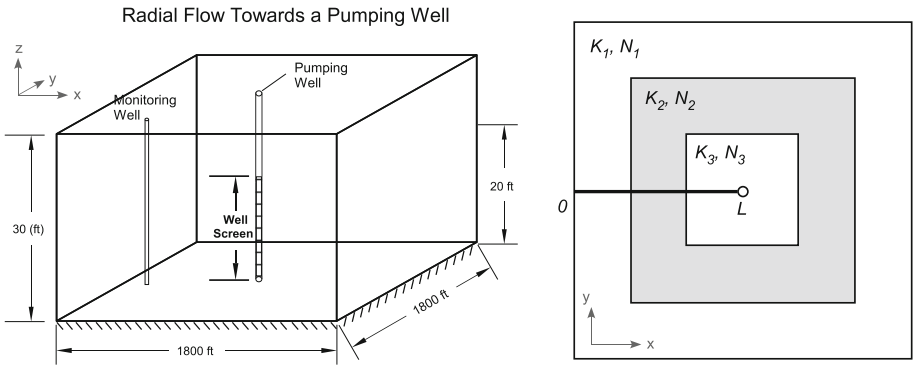

Fig. 3 Schematic diagram of an unconfined aquifer above an impermeable base. A single pumping well operates in the center of the aquifer which is surrounded by a constant head of 20 ft. The inverse domain is shown as a *bold line* in the *right-hand-side figure*, which presents a planeview of the aquifer with a zoned distribution of Ks and Ns. L is the length of the inversion grid. $L = 900$ ft

obtained through Darcy's Law. For the given head datum, the flow rate approximating function is: $\widetilde{Q(x)} = \widetilde{q_x(x)}\widetilde{h(x)}$. Solution of the inverse problem is: $x^{\mathrm{T}} = [a_0^l, a_1^l, K_1, \ldots, K_L]$, where $^{\mathrm{T}}$ denotes transpose, $l = 1, \ldots, G$, G is the number of grid cells.

In test problem 2, a single well pumps water at a constant rate in an aquifer surrounded by constant head boundaries (Fig. 3). The aquifer does not receive recharge. Given the finite problem size, the constant head boundaries impact flow by supplying water to the well. Thus, $\widetilde{h}$ is created by superposing the single-well solution for an infinite aquifer (no boundary effects) with the solution of test problem 1, which describes uniform flow between two constant head reservoirs. This superposition is possible because the flow equation is linear with respect to h^2. Again, vertical flow is ignored and inversion is along a radial axis from the well to the boundary. Solution of the inverse problem is: $x^{\mathrm{T}} = [a_0^l, a_1^l, K_1, \ldots, K_L]$. In this problem, the pumping rate (Q_{w}), considered an observation rather than an unknown, is incorporated into the approximating functions (Table 1). Subsurface Darcy fluxes are not sampled, nor is the hydraulic head at the pumping well. In natural aquifers, head measurements at wells can be subject to wellbore effects (e.g., skin losses, wellbore storage, vertical flows between screened intervals, etc.), which can impart significant measurement errors.

In test problem 3, the forward model is similar to that of test problem 1 (Fig. 2), except that aquifer is receiving recharge at the water table (Table 1). For this problem, Eq. (6) is rewritten to be transmissibility based, and the flow equation becomes linear with respect to hydraulic head. By inverting for T, we aim to understand if the reduced nonlinearity in the flow equation will lead to a different inversion performance, i.e., stability, speed of solver convergence, and accuracy. The flow rate approximating function is again: $\widetilde{Q(x)} = \widetilde{q_x(x)}\widetilde{h(x)}$. The inverse solution is: $x^{\mathrm{T}} = [a_0^l, a_1^l, T_1, \ldots, T_L, N_1, \ldots, N_L]$. Hydraulic conductivity of a hydrofacies is estimated from the transmissibilities: $K = T/\overline{h}^{\mathrm{o}}$, where $\overline{h}^{\mathrm{o}}$ is an average of the observed heads from the hydrofacies.

In test problem 4, a single well pumps water at a constant rate similar to that of test problem 2 (Fig. 3), except aquifer is receiving recharge. Again, the well rate is considered an observation and subsurface fluxes are not sampled. The head at the pumping well is not sampled either. The inverse solution is: $x^{\mathrm{T}} = [a_0^l, K_1, \ldots, K_L, N_1, \ldots, N_L]$.

For all the test problems, though in theory K and N can be discretized at every grid cell, without a large number of measurements, this will result in an underdetermined inversion system of equations. Although nonlinear solvers for underdetermined problems do exist, and similar to many classic inverse methods, one or more regularization constraints can be imposed on the parameters (thus increasing the number of equations), such solutions are not explored here. Instead, all the test problems adopt a deterministic zoned parameterization for both the conductivity and the recharge rate. In addition, the decision to carry out 1D inversion is not a limitation of the inverse method, as analytical solutions exist for 2D and 3D flows for which new problems have been successfully inverted. By presenting a set of 1D analyses, issues of data worth, parameter identifiability, and inversion stability can be clearly illustrated. As long as the Dupuit–Forchheimer assumption (and in the pumping cases, radial symmetry) is satisfied, the 1D analysis reveals how seemingly complex problems can be inverted easily in 1D with small grids.

2.5 Inverse Solution Techniques

Following the steps of Fig. 1, inversion leads to a system of nonlinear equations, $f_i(x)$, $i = 1, \ldots, M$ (M is the number of equations), which can be underdetermined, exact, or overdetermined. For a given problem, the unknowns are the coefficients of the fundamental solutions (Table 1), along with the conductivities and the recharge rates. The system of equations can be minimized using two gradient-based local optimization techniques: Levenberg–Marquardt and Trust-Region-Reflective. Both techniques have been implemented by two nonlinear solvers on Matlab's Optimization Toolbox—*fsolve* and *lsqnonlin* (The Mathworks 2012). For example, *lsqnonlin* solves a (constrained) nonlinear least-squares problem of the form:

$$\min_x \parallel f(x) \parallel_2^2 = \min_x \left(f_1(x)^2 + f_2(x)^2 + \cdots + f_M(x)^2 \right) \tag{7}$$

where x is the solution vector.

With *lsqnonlin*, the equation system can be exact or overdetermined. Constraints can also be placed on x, e.g., enforcing positive conductivities or recharge rates. *fsolve* solves a similar minimization problem, although no constraints can be placed on the solution. *fsolve*'s Levenberg–Marquardt algorithm can also minimize underdetermined problems. Both *fsolve* and *lsqnonlin* require that functions $f_1(x)$, $f_2(x)$, $\ldots$, $f_M(x)$ be continuous over the solution domain. This does not pose a problem because the approximating functions are created by superposing continuous flow solutions.

To use the nonlinear solvers, an initial guess of the solution (x_0) must be provided. x_0 can be estimated in two ways: (1) minimize Eq. (5) with an one-cell inverse grid, excluding the continuity equations, (2) solve an analytical problem assuming an infinite aquifer with homogeneous parameters. Neither approaches require the knowledge of aquifer BC. As an example, for test problem 1, x_0 can be obtained by creating a single-cell inverse grid for which the solution is $x_0^{\mathrm{T}} = [a_0, a_1, K]$. Alternatively, x_0 can be obtained by fitting the analytical solutions ($h^2(x) = a_0 + a_1 x$, $q(x) = -\frac{K a_1}{2\sqrt{a_0 + a_1 x}}$, or $Q(x) = -\frac{K a_1}{2}$) to the observed heads, fluxes, or flow rate (the above solutions also illustrate that unique estimation of K requires at least one flux or flow rate measurement). Moreover, the parameterization adopted for generating x_0 needs not be identical to that of the full inversion, e.g., x_0 can contain a single K even if full inversion estimates a number of Ks. These initial estimates, whether they are obtained with numerical or analytical means, provide a set of physically reasonable parameter values with which the full inversion can be carried out. Because of the homogeneity assumption implicit in the above approaches, data requirement for obtaining x_0 is small.

2.6 Model Structure Errors

Due to the limited subsurface access, inverse parameterization often does not correspond to the true parameter fields, which can result in two types of model structure errors: simplifying and complexifying. For an inverse method to be useful, it is necessary to understand how it performs when its parameterization contains structure errors. For select problems in this study, inverse parameterization is modified from that of the forward model. For example, in test problem 4, the observed data will be sampled from a forward model with multiple Ks and multiple Ns, but inversion only estimates two parameters, assuming uniform K and N over the solution domain. This corresponds to data-poor situations where the underlying parameter variability is unknown. The estimated parameters will be tested for bias by comparing them to an equivalent conductivity (K_{eq}) and an average recharge rate ($\overline{N}$), which are determined from the forward model using mass balance and upscaling techniques (Zhang et al. 2006). Other types of structure error also exist. For the above problem, the inverted parameters can be multiple Ks and a single N (K zonation is known to inversion, but N is assumed homogeneous over the solution domain), or multiple Ns and a single K (N zonation is known, but K is assumed homogeneous). In all these cases, model structure error arises from *simplifying* the true parameter fields. In addition, structure error can arise from *complexifying* the true parameter fields. For example, the forward model does not receive recharge (e.g., test problem 2), but, without data on moisture content, such information may be difficult to infer from limited field data. A modeler may choose to estimate a number of recharge rates by conceptualizing the inversion as that of test problem 4. For this envisioned scenario, several Ns are estimated along with several Ks. The estimated Ns are spurious and how this structure error affects joint estimation of the parameters is also of interest.

3 Results

To verify the inverse solution, a forward model is created for each test problem. In the cross-sectional problems, flow is modeled along a vertical transect, generating observations that can be analyzed in 1D (x axis) under the Dupuit–Forchheimer assumption. After applying the same assumption to the pumping problems, inversion is carried out along the radial axis from the well. A "rule of thumb" was proposed for homogeneous unconfined aquifers, defining the conditions under which the Dupuit–Forchheimer assumption is valid (Haitjema and Mitchell-Bruker 2005):

$$L \gg \sqrt{\frac{K_{\text{H}}}{K_{\text{V}}}} D \tag{8}$$

where K_{H} and K_{V} are horizontal and vertical conductivities ($K_{\text{H}}/K_{\text{V}} = 1.0$ in this work), respectively, L is distance between hydrogeological boundaries (i.e., lateral extent of the forward model), and D is aquifer thickness. Geometry of the forward models is designed following this criterion, which results in negligible vertical flow, even when conductivity is inhomogeneous. Because simultaneous parameter and BC estimation is of interest in this work, boundary effects on flow can be significant. Besides the geometrical constraint placed to satisfy the Dupuit–Forchheimer assumption, each forward model does not adhere to the popular practice of placing the model lateral boundaries far from the center of flow disturbance, i.e., pumping and drawdown. On the contrary, in several problems, BC significantly influence flow.

In the following sub sections, the forward model of each test problem is described, followed by results of the inverse analysis. Some problems are sufficiently simple for which the forward models are analytical solutions; others are more complex, for which the forward models are detailed finite difference solutions by MODFLOW2000. To accurately model well flow with a cartesian grid, the forward model employs local grid refinement at the well. MODFLOW2000 is implemented in the software package Groundwater Vista, which adopts the English unit. Results of this study are presented in: heads and distances (ft), fluxes, conductivities, recharge rates (ft/day or ft/d), and flow rates (ft^3/day or ft^3/d). Alternatively, all dimensional information can be removed, assuming that a consistent set of units is used (Neuman et al. 2007).

To obtain the inverse solutions, the observation data (hydraulic heads, fluxes, or flow rates) are sampled from the forward model and are provided to inversion, which results in the estimation of hydraulic conductivities, recharge rates, and the flow field including the model BC. Compared to test problems 1 and 2, test problems 3 and 4 are more complex with a greater number of parameters, thus stability tests are presented for these problems only. For problems 1 and 2, measurements sampled from the forward models are considered error-free (these data are strictly error-free if the forward model is analytical; they are approximately error-free if the forward model is a finite difference solution). For problems 3 and 4, hydraulic heads sampled from the FDM are corrupted by increasing measurement errors: $h^{\text{measure}} = h^{\text{FDM}} \pm \Delta h$, where Δh is a noise, assigned as 1, 5, and 10 % of the total head variation in the forward model. For example, Δh of 10 % results in a set of head measurements that fluctuate over an interval that is 20 % of the total head change. The larger errors are imposed mainly to test the stability of inversion. Only the measured heads are subject to errors; flow rates or fluxes, when sampled from the forward model, are not affected by errors.

3.1 Test Problem 1: Flow Without Source/Sink Effect

The forward models are a suite of analytical and numerical solutions of unconfined flow between two constant head reservoirs (Fig. 2): $h_0 = 15$ ft and $h_L = 10$ ft. Because there are no source/sink effects, uniform flow from the high head reservoir toward the low head reservoir prevails.

For the given BC, if the aquifer is homogeneous ($K_{true} = 10$ ft/d) with a lateral length (L) of 120 ft, the forward model is solved analytically: $h^2(x) = (1/L)(h_L^2 - h_0^2)x + h_0^2$. (Solutions of q_x and Q_x can also be obtained.) From the forward model, the following observation data are sampled (measurement locations are shown in Fig. 4): (a) 1 head and 1 q_x; (b) 1 head and 1 Q_x; (c) 3 heads and 1 q_x; and (d) 3 heads and 1 Q_x. The inverse grid has 6 cells ($\Delta x = 20$ ft), leading to 10 continuity equations. The inverse systems of equations are thus underdetermined for (a) and (b), and overdetermined for (c) and (d). For each case, the recovered head is plotted and compared to the forward solution (Fig. 4). Compared to $K_{true} = 10$ ft/d, the estimated conductivity is: (a) 15.78, (b) 14.70, (c) 10.00, and (d) 10.00. Clearly, the underdetermined systems, despite being supplied with both head and flux (or flow rate) measurements, lead to inaccurate results, while the overdetermined systems yield correct K estimates and head profiles. For this problem, as few as 4 measurements (with a minimum of one q_x or Q_x) are needed to accurately recover the forward solution. The inverted hydraulic head also extends to the model boundaries, where the boundary heads were not known to inversion. Moreover, q_x and Q_x appear to possess the same information content for estimating the conductivity.

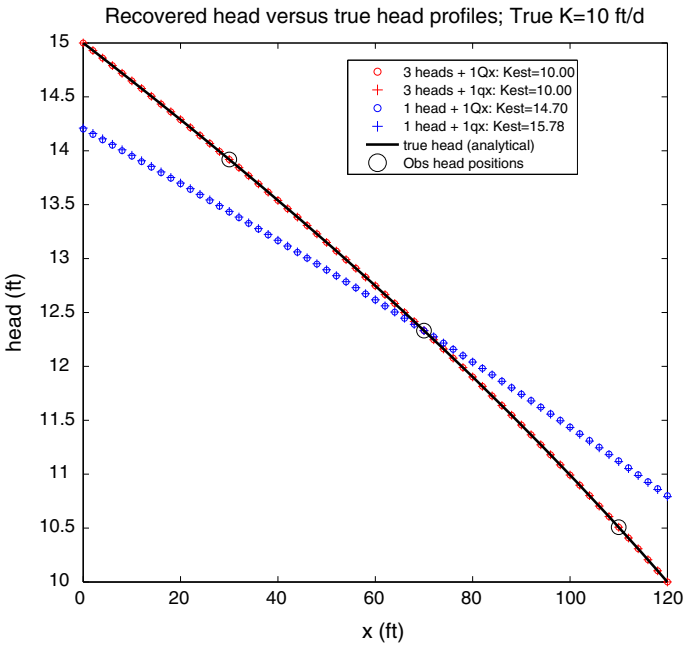

Fig. 4 Inverted heads (*symbols*) and estimated conductivities (K_{est}) for a homogeneous aquifer. The forward solution is shown as *black solid curve*. True conductivity is 10 ft/d. For the cases sampling three heads, measurement location is shown as *large empty circles*. For the cases sampling a single head, this head is measured at $x = 70$ ft. For all cases, flux, or flow rate, is measured at $x = 70$ ft

Next, the forward model is assigned three Ks of equal lateral length (Fig. 2; L is still 120 ft). For the same BC, the forward solution is:

$$h^2(x) = \begin{cases} h_0^2 - c_1 x/[c_2 K_1] & 0 \le x < 40 \\ h_0^2 - c_1 40/[c_2 K_1] - c_1(x-40)/[c_2 K_2] & 40 \le x < 80 \\ h_L^2 + c_1 40/[c_2 K_3] - c_1(x-80)/[c_2 K_3] & 80 \le x \le 120 \end{cases} \tag{9}$$

where $c_1 = h_0^2 - h_L^2$ and $c_2 = \sum_{i=1}^{3} 40/K_a$. For this problem, conductivities are assigned values with increasing contrast, with highest $K_{\max}/K_{\min}$ ratio of 10,000. For a given K distribution, the observed data (hydraulic heads, fluxes, and/or flow rates) are sampled from Eq. (9). In inversion, both a 6-cell ($\Delta x = 20$ ft) and a 24-cell ($\Delta x = 5$ ft) grids are used. For a given inverse grid, problems inverted with 2 observed heads (i.e., two heads, two heads + 1 q_x, two heads + 1 Q_x, two heads + 1 q_x + 1 Q_x) all lead to underdetermined systems of equations; those based on 8 observed heads (or 8 observed heads with flux and/or flow rate measurements) all lead to overdetermined systems of equations. The results of inversion are compiled in Table 2.

Similar to the homogeneous problems, underdetermined systems, despite being supplied with both heads and fluxes (or flow rates), lead to less accurate results. In overdetermined problems, if the 8 observed heads are the only measurements used, the estimated conductivities suffer large errors, but the head recovery is accurate regardless of the conductivity contrast. If one or more q_x (or Q_x) are additionally sampled, conductivity estimations then become accurate. This is expected: unique estimation of K requires head gradient informa-

Table 2 Estimated conductivities (in ft/d) for test problem 1 with three conductivity zones

Parameters:	K_1	K_2	K_3	h_0	h_L
True solution:	10.00	1.00	5.00	15.00	10.00
Low K contrast					
Inverse grid (6 cells)					
Two heads ($x = 40,\ x = 80$)	13.34	12.90	12.84	17.60	4.80
Two heads + $1Q_x$ [a]	1.04	1.00	1.00	17.55	4.80
Two heads + $1q_x$ [b]	1.09	1.05	1.05	17.54	4.81
Two heads + $1Q_x$ [a] + $1q_x$ [b]	10.00	1.00	1.01	15.00	4.93
Eight heads (equal spacing)	27.95	2.79	13.97	**15.00**	**10.00**
Eight heads + $1Q_x$ [a]	10.00	1.00	5.00	**15.00**	**10.00**
Eight heads + $1q_x$ [b]	10.00	1.00	5.00	**15.00**	**10.00**
Eight heads + $1Q_x$ [a] + $1q_x$ [b]	10.00	1.00	5.00	**15.00**	**10.00**
Eight heads + $3Q_x$ [c] + $5q_x$ [c]	10.00	1.00	5.00	**15.00**	**10.00**
True solution:	100.00	10.00	1.00	15.00	10.00
Medium K contrast					
Inverse grid (24 cells)					
Two heads + $1Q_x$ [a]	149.38	9.89	5.60	14.99	13.87
Eight heads (equal spacing)	148.27	14.83	1.48	**15.00**	**10.00**
Eight heads + $1Q_x$ [a]	100.00	10.00	1.00	**15.00**	**10.00**
Eight heads + $3Q_x$ [c] + $5q_x$ [c]	100.00	10.00	1.00	**15.00**	**10.00**
True solution	0.10	10.00	1000.00	15.00	10.00
High K contrast					
Inverse grid (24 cells)					
Two heads + $1Q_x$ [a]	0.21	10.00	2499.8	12.64	10.00
Eight heads (equal spacing)	0.25	25.00	2499.5	**15.00**	**10.00**
Eight heads + $1Q_x$ [a]	0.13	13.14	1297.4	**15.00**	**10.00**
Eight heads + $3Q_x$ [c] + $5q_x$ [c]	0.10	10.00	1000.00	**15.00**	**10.00**

Boundary heads (in ft) are shown as h_0 and h_L. When the recovered head profile is identical to the forward solution, h_0 and h_L are shown in bold font

[a] Q_x is sampled at the outflow boundary at x = 120 ft

[b] q_x is sampled at x = 70 ft

[c] Q_x is sampled at x = 0, 60, 120 ft; q_x is sampled at x = 30, 40, 70, 80, 110 ft

tion as embodied in the flux or flow rate data, in addition to hydraulic head measurements. Furthermore, when the conductivity contrast increases, given the same observed data (e.g., 8 heads + $1Q_x$), conductivities of the medium- to high-K-contrast problems suffer greater errors. In this case, adding more data (e.g., 8 heads + $3Q_x + 5q_x$) leads to more accurate K estimates.

Inversion is further tested on a problem with the same BC, but the aquifer bottom is not flat (Fig. 2; $L = 900$ ft, aquifer thickness is 30 ft, and $H = 8.5$ ft). For different K distributions of increasing contrasts, 2D finite difference forward simulations are carried out with these parameters: $\Delta x = \Delta y = 1$, $\Delta z = 0.5$, $N_x = 900$, $N_y = 1$, $N_z = 60$, where N_x, N_y, N_z are the number of grid cells along the x, y, z axes, respectively. To represent the triangular aquifer

Table 3 Estimated conductivities for test problem 1 with a triangular aquifer bottom

	Homogeneous Inverse grid (24 cells)				Low K contrast Inverse grid (6 cells)		
Parameters: True solution:	K 5.00				K_1 10.00	K_2 1.00	K_3 5.00
Nine heads + 3 q_x	4.71			Nine heads + 3q_x	12.20	1.06	3.42
Nine heads + 3 q_x + 2 Q_x	4.60			Nine heads + 3q_x + 3Q_x	9.99	0.73	2.72
	Medium K contrast Inverse grid (24 cells)				High K contrast Inverse grid (24 cells)		
Parameters: True solution:	K_1 100.00	K_2 10.00	K_3 1.00		K_1 0.10	K_2 10.00	K_3 1,000.00
Nine heads + 3q_x	292.57	9.28	0.91	Twelve heads + 3q_x + 3 Q_x	0.36	6.56	921.5
Eleven heads + 3q_x [a]	99.80	9.34	0.91	Twelve heads + 4q_x [b] + 3Q_x	0.36	6.56	989.3

In most of these problems, head, q_x, and Q_x sampling is semi-regular over the 900 ft inversion domain
[a] Adding 3 Q_x measurements first did not improve the solution (not shown). When 2 additional heads are sampled in the K_1 zone (at $x = 150.5$ and 290.5 ft), K_1 estimation improves significantly
[b] An additional q_x is sampled in the K_3 zone, leading to an improved K_3 estimate

bottom, inactive cells are assigned beneath the triangle. For all K distributions, global mass balance errors of the forward models are less than 0.1 %, numerical errors in the observed data sampled from these models are thus considered small. The inverse solutions are summarized in Table 3, one for each K distribution. For all distributions, head recovery is very good and is not presented. Despite violation of the Dupuit–Forchheimer assumption (i.e., due to the 8.5 ft rise of the aquifer bottom in the model center, appreciable vertical flow is observed in the forward models), conductivity estimations are reasonably accurate. Additional sampling of heads or fluxes within a hydrofacies zone further improves the estimation accuracy of the hydrofacies conductivity.

3.2 Test Problem 2: Flow With a Pumping Well (No Areal Recharge)

For a set of four K distributions with increasing contrasts, the forward model (1,800 × 1,800 × 30 ft^3) is simulated with a no-flow boundary at the bottom and a specified head of 20 ft along the sides (Fig. 3). The top boundary (water table) is solved iteratively by MODFLOW2000 using convertible layers. Areal recharge is not applied. A single pumping well, with a constant discharge rate, induces radial flow toward the model center. For each K distribution, Q_w is adjusted to ensure that hydraulic head at the well will not drop below the top of the well screen (screen length is adjusted as well). The forward model initially employs a coarse grid ($N_x = 60$, $N_y = 60$, $N_z = 60$), before it is refined at the pumping well and at the interfaces between hydrofacies. With the refined grid, global mass balance errors are less than 0.1 % for all K distributions. From the forward models, hydraulic heads are sampled quasi-regularly along the radial axis at an elevation of 3.5 ft. Darcy fluxes are not sampled, nor is the head at the pumping well. The well rate is considered known and is incorporated into the inverse formulation. Inversion is carried out along the same radial axis.

For a case with low K contrast ($K_1 = 5$, $K_2 = 1$, and $K_3 = 10$), a preliminary inversion is carried out with ten observed heads using a 24-cell, grid ($\Delta x = 37.5$ ft). Result is inaccurate: (1) the estimated conductivities contain up to 100 % errors; (2) the recovered head at the pumping well, exhibits the largest deviation from the true head (smallest head deviation

Table 4 Estimated conductivities for test problem 2 with three conductivity zones and a pumping well which lies in the center of the K_3 zone (see Fig. 3)

	Low K contrast $Q_w = 250$ ft^3/d					Medium K contrast $Q_w = 250$ ft^3/d			
Parameters:	K_1	K_2	K_3	h_{well}		K_1	K_2	K_3	h_{well}
True solution:	5.00	1.00	10.00	17.65		1.0	10.00	100.00	19.10
Eleven heads + Q_w	5.14	0.97	11.50	17.67	Eleven heads + Q_w	1.11	9.98	113.53	19.08
					Eleven heads + Q_w + 3q_x[a]	0.96	14.57	126.44	19.08
	Medium K contrast $Q_w = 125$ ft^3/d					High K contrast $Q_w = 125$ ft^3/d			
Parameters:	K_1	K_2	K_3	h_{well}		K_1	K_2	K_3	h_{well}
True solution:	10.00	100.0	1.00	15.20		1,000.00	0.10	10.00	11.30
Eleven heads + Q_w	11.14	88.10	1.15	15.23	Eleven heads + Q_w	1204.3	0.10	11.48	11.26
Twenty heads[b] + Q_w	11.17	103.62	1.19	15.23	Twenty heads + Q_w	698.64	0.12	10.70	11.26

h_{well} is hydraulic head at the pumping well
[a] Three q_x measurements are made at the inflow boundary, near the pumping well, and in between;
[b] Sampling density for heads is doubled, with the sampling location following the same semi-regular pattern

occurs at the constant head boundary). The inverse grid is then refined: the previous 24th cell, located closest to the pumping well, is split into: cell 24 ($\Delta x = 18.75$ ft), cell 25 ($\Delta x = 9.375$ ft), and cell 26 ($\Delta x = 9.375$ ft). Given the same observed data, both the estimated conductivities and the recovered head profile improve immediately.

With the refined (26-cell) grid, the estimated conductivities are listed in Table 4, along with the recovered heads at the pumping well. For a case with medium K contrast, K values are also switched: the pumping well first lies in a high-K zone ($K_3 = 100$ ft/d), and then in a low-K zone ($K_3 = 1$ ft/d). In all cases, head recovery is excellent, while the estimated conductivities are reasonably accurate. Given the same observations, the highest-K-contrast case suffers the greatest K estimation errors, similar to what was observed for test problem 1. Moreover, when K contrast increases, or when the pumping well lies in a low-K zone, well rate is adjusted lower so as not to dewater the aquifer at the well screen. Head variation, from a high of 20 ft at the boundary to the lowest value at the well, changes accordingly: it is less than 3 ft for the case with a low K contrast, but rises to 9 ft for the case with a high K contrast. Despite this difference in drawdown, conductivity estimation and hydraulic head recovery are not affected. Data quantity, on the other hand, appears to be more important for the estimation accuracy.

3.3 Test Problem 3: Flow With Areal Recharge (No Pumping)

The forward model is similar to test problem 1 (Fig. 2; L is now 900 ft). Areal recharge is applied to the water table throughout the model. Initially, a uniform recharge rate is assigned ($N = 0.005$ ft/d), along with these parameters and BC: $h_0 = 15$ ft, $h_l = 10$ ft, $K_1 = 30$ ft/d, $K_2 = 100$ ft/d, $K_3 = 10$ ft/d. The same finite difference grid of test problem 1 is used, except here the aquifer bottom is flat. Because of the recharge, water table builds up near the model center, where a hydrological divide occurs at $x \simeq 300$ ft, and diminishes toward the boundaries. From the forward model, 8 hydraulic heads, 2 Q_x, and 4 q_x are sampled semi-regularly at a fixed elevation.

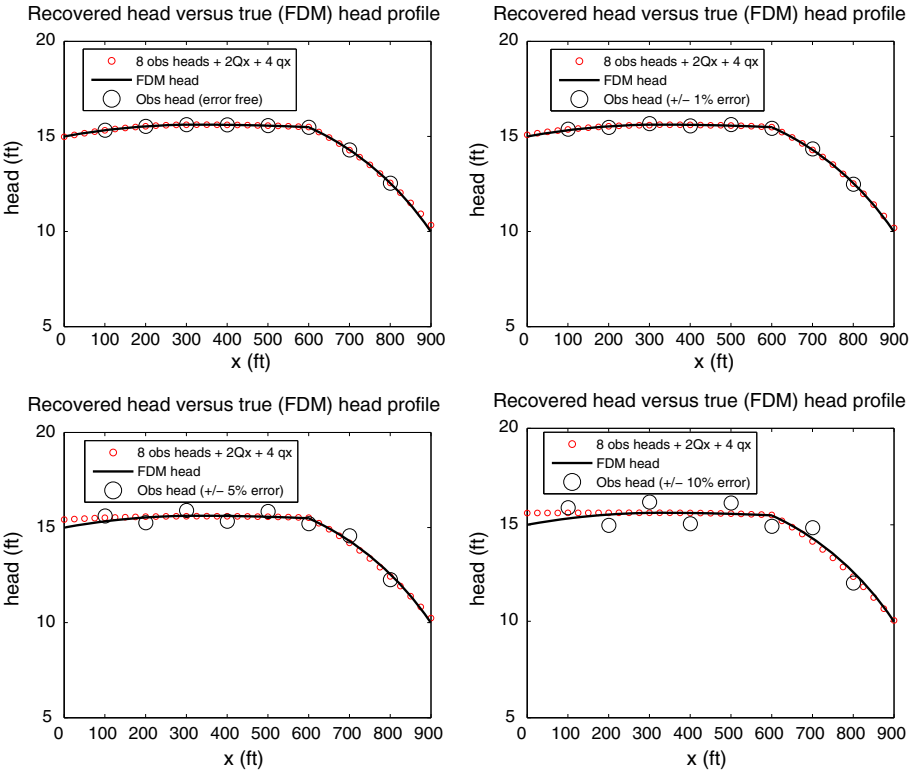

Fig. 5 Recovered head profiles (*red circles*) of test problem 3 under increasing measurement errors. Location of the observed heads is indicated by *large empty circles*. The forward solution is shown as *black solid curve*. The inverse grid has six cells ($\Delta x = 150$)

In inversion, a grid with six cells is used, using the approximating functions of in Table 1. Given error-free observed data, inversion yields: (1) nearly perfect recovery of the hydraulic head profile compared to the true water table (Fig. 5); (2) $T_1 = 463.75$ ft^2/d or $K_1 = 30.12$ ft/d; (3) $T_2 = 1672.20$ ft^2/d or $K_2 = 107.34$ ft/d; (4) $T_3 = 142.56$ ft^2/d or $K_3 = 10.76$ ft/d; and (5) $N = 0.0064$ ft/d. The estimated parameters are close to their true values. Next, this problem is inverted by setting $Q_w = 0$ in the inverse code of test problem 4 (see Sect. 3.4), which directly estimates the conductivities. Besides yielding nearly identical inversion results, both codes have a similar solver performance, i.e., number of iterations needed to achieve convergence and solver speed. Inversion accuracy and solver performance are therefore not sensitive to the degree of nonlinearity in the inverse formulation.

Measurement errors (± 1 %) are then added to the observed heads, leading to these results: (1) nearly perfect head recovery (Fig. 5); (2) $K_1 = 35.69$ ft/d; (3) $K_2 = 93.38$ ft/d; (4) $K_3 = 10.82$ ft/d; and (5) $N = 0.0068$ ft/d. When ± 5 % errors are used, inversion yields: (1) fairly good head recovery with the leftmost heads slightly overestimated (Fig. 5); (2) $K_1 = 105.32$ ft/d; (3) $K_2 = 173.98$ ft/d; (4) $K_3 = 10.08$ ft/d; (5) $N = 0.0056$ ft/d. When ± 10 % errors are used, inversion yields: (1) reasonably accurate head recovery (Fig. 5); (2) $K_1 = 1457.30$ ft/d; (3) $K_2 = 114.31$ ft/d; (4) $K_3 = 9.73$ ft/d; (5) $N = 0.0056$ ft/d. Clearly, parameter estimation error increases with increasing measurement error. Compared to the estimated recharge rate and head recovery, K estimation is more sensitive to the measurement

errors. Moreover, K_1 is consistently overestimated as a result of the specific measurements used and their specific errors. For the case with ± 10 % errors, if error signs are switched among the observed heads, inversion yields: (1) $K_1 = 12.59$ ft/d; (2) $K_2 = 85.12$ ft/d; (3) $K_3 = 11.57$ ft/d; (4) $N = 0.0056$ ft/d. K_1 is now underestimated, while the recovered head near the left boundary (not shown) slightly underestimates the true water table.

Next, the forward model is rerun with spatially variable recharge: $N_1 = 0.005$ ft/d, $N_2 = 0.0167$ ft/d, $N_3 = 0.00167$ ft/d. The recharge zones are identical to the conductivity zones. From this model, 17 heads, $3Q_x$, and $5q_x$ are sampled in a semi-regular pattern. With error-free data, inversion yields: (1) perfect head recovery (not shown); (2) $K_1 = 31.02$ ft/d; (3) $K_2 = 94.15$ ft/d; (4) $K_3 = 10.64$ ft/d; (5) $N_1 = 0.007$ ft/d; (6) $N_2 = 0.0164$ ft/d; and (7) $N_3 = 0.0065$ ft/d. With the exception of N_3, all parameters are accurately estimated. When measurement errors are increased, inverse solutions behave similarly to those observed previously for the problem with uniform recharge: inversion is stable under increasing errors, but accuracy of the estimated parameters degrades.

Finally, from the same forward model (i.e., three Ks and three Ns), a new set of observations—8 heads, 2 Q_x, and 4 q_x, are sampled. Inversion adopts a simplified parameterization, whereby three Ks and a single N are estimated, yielding: (1) perfect head recovery (not shown); (2) $K_1 = 30.48$ ft/d; (3) $K_2 = 107.82$ ft/d; (4) $K_3 = 9.53$ ft/d; and (5) $N = 0.0072$ ft/d. The estimated N is close to the mean aquifer recharge rate: 0.0078 ft/d. Despite this structure error, accuracy of the simultaneously estimated conductivities is not affected. In addition, stability tests under increasing measurement errors are conducted, yielding similar behaviors as those observed for problems without structure errors.

3.4 Test Problem 4: Flow With Areal Recharge and A Pumping Well

The forward model is similar to test problem 2 (Fig. 3), except areal recharge is additionally applied to the water table. The same finite difference grid of test problem 2 is used, containing grid refinement at the pumping well and at the hydrofacies interfaces. Except for the recharge boundary, BC are identical to those of test problem 2. The true conductivities are: $K_1 = 10$ ft/d, $K_2 = 100$ ft/d, and $K_3 = 30$ ft/d. Initially, uniform recharge is applied at the top boundary, and then, nonuniform recharge. In both cases, a steady-state pumping rate of 3,000 ft^3/d can be maintained. Because of the recharge, flow pattern is complex in both cases though it is still radially symmetric: near the pumping well, converging flow is observed; away from the well, water table builds up in a circular mound, where recharge water on the inner side of the divide flows toward the well, and that on the outer side flows toward the boundary. From the forward model, 19 heads are sampled semi-regularly at a fixed elevation, from the well toward the boundary. In inversion, conductivity-based formulations are adopted (Table 1), leading to the following results:

When a uniform recharge is applied to the forward model, inversion recovers the hydraulic heads, the three conductivities, and the single N (not shown), with a similar level of accuracy as that of test problem 3. Stability analysis is also conducted, with similar error characteristics as those of test problem 3.

When nonuniform recharge is applied (true $N_1 = 0.005$ ft/d, $N_2 = 0.025$ ft/d, and $N_3 = 0.010$ ft/d), an initial guess of the solution is obtained with error-free observations (i.e., 19 heads and Q_w) using an one-cell inverse grid: $K_1 = 11.35$ ft/d; $K_2 = 22.78$ ft/d; $K_3 = 21.84$ ft/d; $N_1 = 0.0214$ ft/d; $N_2 = 0.0078$ ft/d; $N_3 = 0.0125$ ft/d; and $a_0 = 556.79$. Interestingly, though these parameters are far from accurate, the recovered hydraulic head profile (not shown), which spans the single cell, nearly perfectly matches the forward solution. Given this initial guess, inversion with the 26-cell grid (i.e., the same as that of test problem

2, with local grid refinement at the well) yields: (1) nearly perfect head recovery (Fig. 6); (2) $K_1 = 12.17$ ft/d; (3) $K_2 = 103.69$ ft/d; (4) $K_3 = 21.26$ ft/d; (5) $N_1 = 0.023$ ft/d; (6) $N_2 = 0.021$ ft/d; and (7) $N_3 = 0.013$ ft/d. With the exceptions of N_1 and K_3, most parameters are accurately estimated. Moreover, different x_0 were generated with the one-cell inversion by adopting different parameterizations, e.g., inverting K_1, K_2, K_3, and a single N, or inverting a single K and a single N. The subsequent full inversions yield identical results as those for which x_0 contains all 6 parameters. Clearly, for the given measurements, the inverse problem is well-posed, leading to unique solutions that are insensitive to the choice of x_0. Moreover, inversion stability is tested with measurement errors up to ± 10 % of the total head variation. Similar behaviors as those reported above for test problem 3 and for test problem 4 with uniform recharge are observed. Even with the largest errors, solution is stable, although accuracy of the estimated parameters degrades.

3.5 Grid Refinement

Previous experimentations with the inverse grid suggest that, for a given set of measurements, local grid refinement in the high head gradient region (i.e., near the well) can improve the inversion accuracy. However, this is true only to a certain extent. For example, for test problem 4 with three Ks and three Ns, given the same error-free data (19 heads and Q_w), inversion with a 52-cell grid (i.e., the 26-cell grid is uniformly refined) did not improve the results. The estimated parameters are: (1) nearly perfect head recovery; (2) $K_1 = 11.00$ ft/d; (3) $K_2 = 93.54$ ft/d; (4) $K_3 = 20.99$ ft/d; (5) $N_1 = 0.021$ ft/d; (6) $N_2 = 0.019$ ft/d; and (7) $N_3 = 0.014$ ft/d, which do not differ significantly from those obtained using the coarser grid. On the other hand, for a fixed inverse grid, increasing measurements generally leads to more accurate results, as discussed above. Clearly, both inverse grid discretization and data density affect the inversion accuracy.

3.6 Model Structure Errors

For test problem 4 with 3 Ks and 3 Ns, despite the existence of converging and diverging flows, groundwater in the forward model is largely perpendicular to the conductivity zones. Assuming an infinitely acting aquifer, an approximate lateral equivalent conductivity (K_{eq}) can be calculated analytically as 20.93 ft/d, a harmonic average of K_1, K_2, and K_3. Using area-weighted mean of $N1$, $N2$, and $N3$, an average recharge rate is estimated at 0.012 ft/d. Based on same error-free measurements (i.e., 19 heads and Q_w), the same 26-cell grid, conductivities and recharge rates are re-estimated with the inverse parameterization containing simplifying structure errors:

- A single K and a single N are estimated. In this case, head recovery is reasonably accurate (Fig. 6). The estimated parameters are: $K = 12.88$ ft/d, $N = 0.016$ ft/d. K underestimates K_{eq}, but N is close to the average recharge rate.
- Three conductivities and a single N are estimated. Head recovery is accurate (Fig. 6). The estimated parameters are: $K_1 = 7.84$ ft/d, $K_2 = 67.66$ ft/d, $K_3 = 20.92$ ft/d, and $N = 0.015$ ft/d. The estimated recharge rate is close to the average value, while the estimated conductivities are similar to those of test problem 4 without model structure error (see Sect. 3.4). The accuracy of conductivity estimation is not affected by the incorrect recharge parameterization.
- Three recharge rates and a single K are estimated. Head recovery is again accurate (Fig. 6). The estimated parameters are: $K = 18.58$ ft/d, $N_1 = 0.033$ ft/d, $N_2 = 0.0089$ ft/d, and $N_3 = 0.014$ ft/d. The estimated conductivity is not far from K_{eq}. The estimated recharge

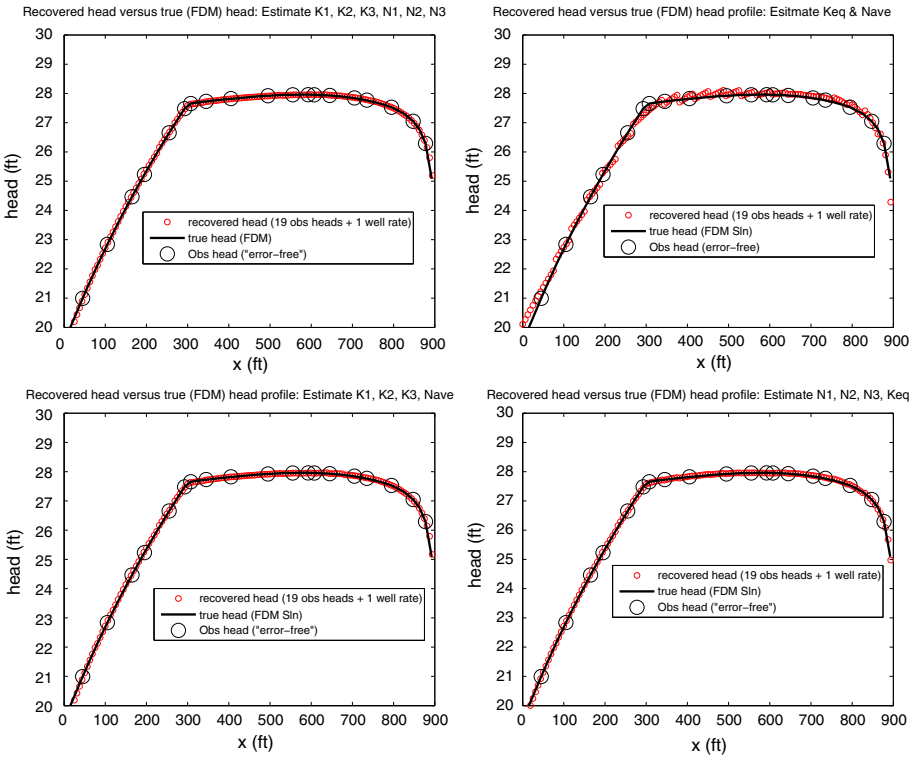

Fig. 6 Recovered head profiles (*red circles*) of test problem 4 with different inverse parameterizations. The forward model has three K zones and three N zones (Fig. 3), with the true water table shown as *black solid line*. The pumping well is located at $x = 900$ ft. The observed heads are error-free, with their location indicated by *large empty circles*. K_{eq} is a single K estimated by inversion; N_{ave} is a single recharge rate estimated by inversion

rates are similar to those of test problem 4 without model structure error. The accuracy of recharge estimation is not affected by the incorrect conductivity parameterization.

The above results suggest that hydraulic head (therefore boundary head) estimation can be accurate even if the inverse formulation contains various parameterization errors. Despite these errors, inversions are stable and the estimated parameters are physically reasonable, i.e., they are comparable to the analytical equivalent or average parameters. Because only limited observations are used to condition the inverse solution, the estimated parameters will not generally be identical to the equivalent or average values obtained with perfect knowledge. In addition, when structure error exists for one parameter, estimation accuracy of the other parameter with correct parameterization is not affected. When both recharge and conductivity are incorrectly parameterized, the estimated parameters are still reasonable.

Next, complexifying structure error is investigated. For example, when the inverse formulation contains the recharge term, what will happen to its solution if the actual recharge is zero? Test problem 4 is inverted again, but the forward model is assigned zero recharge, while maintaining the same pumping rate. From this model, the same 19 error-free heads are sampled. Inversion with the 26-cell grid yields excellent head recovery (not shown), with these estimated parameters: (1) $K_1 = 14.08$ ft/d; (2) $K_2 = 89.70$ ft/d; (3) $K_3 = 23.88$ ft/d; (4) $N_1 = -1.8 \times 10^{-4}$ ft/d; (5) $N_2 = 5.8 \times 10^{-5}$ ft/d; and (6) $N_1 = 8.2 \times 10^{-4}$

ft/d. The three estimated recharge rates are extremely small, pointing to the error in recharge parameterization. This result can also lead to a more parsimonious future model, e.g., inverse parameterization can be simplified after new data are collected to confirm the structure error. The error in parameterizing recharge similarly does not affect the simultaneous estimation of the conductivities, i.e., all Ks are comparable to those found for test problem 4 without model structure error (see Sect. 3.4).

4 Discussion

The new inverse method, similar to all inversion techniques, can suffer ill-posedness when insufficient or inaccurate data are provided. Thus, (1) solution may not exist; (2) solution may not be unique; and (3) solution may be unstable. These issues are explored in this work by inverting a set of test problems for which observations of different types, quantities, and qualities are used as conditioning data. Results suggest that exact or overdetermined inversion systems of equations can lead to stable solutions, but the accuracy of the estimated parameters (i.e., hydraulic conductivities and recharge rates) is affected by the type of measurements used and their errors. When the observed data are of the right type (i.e., both heads and a minimum of one Darcy flux or one flow rate), are of sufficient quantity (i.e., the inverse equation system is exact or overdetermined), and do not contain extremely large errors, the inverse problem becomes well-posed, which leads to unique and accurate estimation of the parameters, flow field, and BC. However, if only hydraulic heads are available, inversion can accurately recover the head solution throughout the model domain (thus the boundary heads), but cannot uniquely estimate the parameters. This is expected given our earlier discussion in Introduction about the parameter identifiability issue. Moreover, for well-posed problems, starting the full inversion with different initial guesses generally yields identical outcomes with fast solver convergence. For various unconfined problems subject to different source/sink effects, the inverse method is shown to be robust and efficient:

- By providing as few as one pumping rate in addition to hydraulic heads, multiple Ks and Ns can be uniquely and simultaneously estimated, along with the model flow field and BC. This demonstrates that inversion can succeed for heterogeneous problems as long as a single head-gradient-based measurement is provided. Data requirement of the method is low.
- Inversion result is stable with increasing measurement errors (up to $\pm 10\,\%$ of the total head variation). As measurement error increases, parameter estimation becomes less accurate, as expected;
- Inversion is computationally efficient. For well-posed problems, convergence time on a PC workstation is typically a few seconds. For problems that are not well-posed (e.g., lacking flux or flow rate measurement, underdetermined equations due to insufficient data), the method typically does not converge, no matter how stringent the solver convergence criteria are (in these cases, parameter estimates are those obtained at the maximum solver iteration);
- Inversion accuracy is relatively insensitive to parameter variability, e.g., $K_{\max}/K_{\min}$ is successfully tested up to 10,000. However, for a given problem, when $K_{\max}/K_{\min}$ increases, more observation data are needed to achieve the same accuracy. Inversion accuracy is also insensitive to the transmissibility versus conductivity-based formulations. In the latter formulation, the approximating functions are more strongly nonlinear;

– Inversion accuracy is insensitive to flow patterns. The flow path, as long as it is largely horizontal, can be unidirectional (test problem 1), convergent (test problem 2), divergent (test problem 3), and quite complex with converging and diverging flows (test problem 4). This suggests that by developing approximating functions that superpose individual well solutions, the method can address problems with multiple injection and production wells. This has been confirmed by successfully inverting a 2D problem with four conductivities, two recharge rates, and a pair of well dipole.
– Despite the Dupuit–Forchheimer assumption with which the inverse formulation is developed, inversion accuracy is not significantly affected by minor violation of this assumption, suggesting a broader applicability of these solutions to aquifers with irregular shapes.

The inverse method is developed using analytical unconfined flow solutions in idealized situations, i.e., wellbore radius is assumed zero and vertical flow in the aquifer is considered negligible. Caution is needed when applying the method to real aquifers, where additional effects, such as wellbore storage, partial penetration, or skin losses (not all such effects can be accounted for by the forward model) can affect the accuracy of the observed data and, therefore, inversion accuracy. Vertical flow can be significant near barriers such as impervious faults or subsurface engineered structures. Future work is needed to precisely define the conditions where non-negligible vertical flow may significantly impact the accuracy of inversion. For such problems, higher dimensional techniques explicitly accounting for vertical flow are needed.

In this work, parameter zonation is known to inversion, leading to a set of solutions without uncertainty measures. The zonation pattern, in effect, enforces a deterministic constraint on the parameters. To remove this constraint and to account for static data uncertainty, the inverse method can be integrated with geostatistics, whereby uncertainty in both the estimated parameters and the estimated state variables (including model BC) can be quantified (Wang et al. 2013). Because analytical solutions are used to generate the approximating functions, future work can explore inverting such solutions within a stochastic framework, i.e., conductivity and recharge become spatial random functions. Moreover, though the current method adopts a zoned parameterization, whereby the number of parameters is small compared to the number of observations, future work can explore highly parameterized inversion for which regularization (e.g., smoothness constraint, spatial covariances, cross correlation between hydrological parameters and geophysical measurements) can be incorporated into the inversion equations. The additional constraints will allow us to solve for a larger number of parameters, e.g., one K at each inverse grid cell. Finally, the inverse method does not explicitly account for unsaturated flow process which is treated as an instantaneous recharge to the water table. There is a growing body of work that couples and inverts flow in the unsaturated and saturated zones for which parameters specific to each zone are estimated (Moench 2004; Mishra and Neuman 2010, 2011; Mao et al. 2013). Whether or not the continuity concept of this study can be extended to unsaturated flow and coupled processes will require further investigations. For such problems, data requirement to obtain well-posed inversion is likely higher (Mao et al. 2013).

5 Conclusion

A physically-based inverse method is developed to analyze steady-state flow in an unconfined aquifer with heterogeneous hydraulic conductivities and significant source/sink effects. The method extends the confined aquifer inversion of Irsa and Zhang (2012), where a single con-

ductivity and model boundary conditions were estimated for problems without source/sink effects. In this work, to address nonlinearity in the unconfined flow equation, the hydraulic head approximating function is created by superposing analytical flow solutions for homogeneous sub-domains. Given appropriate measurements, the inversion system of equations becomes well-posed and can be solved with nonlinear optimization, which allows the simultaneous estimation of multiple conductivities and recharge rates. From the inverse solution, the flow field including the unknown BC can be recovered. Because the inverse method does not optimize any objective functions (i.e., data-model mismatch) which require forward flow simulations, the method is computationally efficient.

Under the Dupuit–Forchheimer assumption, accuracy and stability of the method are demonstrated by inverting heterogeneous synthetic aquifer problems with increasingly complex flow: (1) aquifer domains without source/sink effects; (2) aquifer domains with a point sink (a pumping well operating under a constant discharge rate); (3) aquifer domains with constant or spatially variable recharge; (4) aquifer domains with constant or spatially variable recharge undergoing single-well pumping. In the problems without the pumping well, observation data are hydraulic heads, Darcy fluxes, and/or flow rates; in the problems with the pumping well, the observation data are hydraulic heads and the pumping rate. For all problems, inverse solutions are stable under increasing measurement errors, although accuracy of the estimated parameters degrades with increasing errors. The method is successfully tested on strongly heterogeneous problems with conductivity contrast up to 10,000.

The inverse problem must be well-posed to obtain accurate solutions, i.e., the observation data must be of sufficient quantity, adequate quality, and of the necessary types. For example, given only head measurements, inversion can yield accurate head profiles extending to the model boundaries. Accurate estimation of the conductivities and the recharge rates, however, requires both hydraulic head and Darcy flux or flow rate measurements. Interestingly, a single flux or flow rate measurement suffices to enable the unique and simultaneous estimation of multiple conductivity and recharge parameters. Inversion accuracy is also affected by the resolution of the inverse grid: at locations where hydraulic head gradient is large, local grid refinement can improve the solution. Moreover, the inverse method obviates the well-known issue associated with model "structure errors," whereas inverse parameterization simplifies or complexifies the true parameter field. For several heterogeneous problems, when aquifer is assumed homogeneous with a constant recharge, physically meaningful parameter estimates (i.e., equivalent conductivities and mean recharge rates) can be obtained. Alternatively, if the inverse parameterization contains spurious parameters, inversion can identify such parameters, while the simultaneous estimation of non-spurious parameters is not affected.

Acknowledgments This research is supported by the University of Wyoming Center for Fundamentals of Subsurface Flow (WYDEQ49811ZH). The author acknowledges helpful comments of two anonymous reviewers who helped to improve the content and organization of this paper.

References

Bear, J.: Dynamics of Fluids in Porous Media, vol. 764, 1st edn. Elsevier, New York (1972)

Bouwer, H., Rice, R.C.: A slug test for determining hydraulic conductivity of unconfined aquifers with completely or partially penetrating wells. Water Resourc. Res. **12**(3), 423–428 (1976)

Cardiff, M.: W, B., Kitanidis, P., Malama, B., Revil, A., Straface, S., Rizzo, E.: A potential-based inversion of unconfined steady-state hydraulic tomography. Ground Water **47**(2), 259–270 (2009)

Carrera, J., Neuman, S.P.: Estimation of aquifer parameters under transient and steady state conditions: III. Application to synthetic and field data. Water Resourc. Res. **22**(2), 228–242 (1986)
Cooley, R.L., Christensen, S.: Bias and uncertainty in regression-calibrated models of groundwater flow in heterogeneous media. Adv. Water Resourc. **29**(5), 639–656 (2005)
Cooper, H.H., Bredehoeft, J.D., Papadopulos, I.S.: Response of a finite-diameter well to an instantaneous charge of water. Water Resourc. Res. **3**, 263–269 (1967)
Crisman, S.A., Molz, F.J., Dunn, D.L., Sappington, F.C.: Application procedures for the electromagnetic borehole flowmeter in shallow unconfined aquifers. Groundw. Monit. Remediat. **12**(3), 96–100 (2007)
Dagan, G.: A method determining the permeability and effective porosity of unconfined anisotropic aquifers. Water Resourc. Res. **3**(4), 1059–1071 (1967)
Dagan, G.: A note on packer, slug, and recovery tests in unconfined aquifers. Water Resourc. Res. **14**, 929–934 (1978)
Darnet, M., Marquis, G., Sailhac, P.: Estimating aquifer hydraulic properties from the inversion of surface streaming potential (SP) anomalies. Geophys. Res. Lett. **30**(13), 1679 (2003). doi:10.1029/2003GL017631
Day-Lewis, F., Lane, J.W., Gorelick, S.M.: Combined interpretation of radar, hydraulic, and tracer data from a fractured-rock aquifer. Hydrogeol. J. **14**(1–2), 1–14 (2006)
Dettinger, M.D.: Reconnaissance estimates of natural recharge to desert basins in Nevada, U.S.A., by using chloride-balance calculations. J. Hydrol. **106**, 55–78 (1989)
Doherty, J., Welter, D.: A short exploration of structure noise. Water Resourc. Res. **46**, W05525 (2010). doi:10.1029/2009WR008377
Fienen, M., Hunt, R., Krabbenhoft, D., Clemo, T.: Obtaining parsimonious hydraulic conductivity fields using head and transport observations: A Bayesian geostatistical parameter estimation approach. Water Resourc. Res. **45**, W08405 (2009). doi:10.1029/2008WR007431
Gaganis, P., Smith, L.: Accounting for model error in risk assessments: Alternative to adopting a bias towards conservative risk estimates in decision models. Adv. Water Resourc. **31**(8), 1074–1086 (2008)
Haitjema, H.M., Mitchell-Bruker, S.: Are water tables a subdued replica of the topography? Ground Water **43**(6), 781–786 (2005)
Hantush, M.S., Jacob, C.E.: Non-steady radial flow in an infinite leaky aquifer. Trans. Am. Geophys. Union **36**(1), 95–100 (1955)
Harvey, C.F., Gorelick, S.M.: Mapping hydraulic conductivity: Sequential conditioning with measurements of solute arrival time, hydraulic head, and local conductivity. Water Resourc. Res. **31**(7), 1615–1626 (1995)
Healy, R.W., Cook, P.: Using groundwater levels to estimate recharge. Hydrogeol. J. **10**(10), 91–109 (2002)
Hill, M.C., Tiedeman, C.R.: Effective Groundwater Model Calibration: With Analysis of Data, Sensitivities, Predictions, and Uncertainty, vol. 480, 1st edn. Wiley-Interscience, Berlin (2007)
Irsa, J., Zhang, Y.: A new direct method of parameter estimation for steady state flow in heterogeneous aquifers with unknown boundary conditions. Water Resourc. Res. **48**, W09526 (2012). doi:10.1029/2011WR011756
Jyrkama, M.I., Sykes, J.F., Norman, S.D.: Recharge estimation for transient ground water modeling. Ground Water **40**(6), 638–648 (2002)
Keating, E.H., Doherty, J., Vrugt, J.A., Kang, Q.: Optimization and uncertainty assessment of strongly nonlinear groundwater models with high parameter dimensionality. Water Resourc. Res. **46**, W10517 (2010). doi:10.1029/2009WR008584
Li, W., Englert, A., Cirpka, O.A., Vereecken, H.: Three dimensional geostatistical inversion of flowmeter and pumping test data. Ground Water **46**(2), 193–201 (2008)
Lin, Y.F., Wang, J., Valocchi, A.: PRO-GRADE: GIS toolkits for ground water recharge and discharge estimation. Ground Water **47**(1), 122–128 (2009)
Liu, G., Chen, Y., Zhang, D.: Investigation of flow and transport processes at the MADE site using ensemble Kalman filter. Adv. Water Resourc. **31**, 975–986 (2008)
Liu, X., Kitanidis, P.: Large-scale inverse modeling with an application in hydraulic tomography. Water Resourc. Res. **47**, W02501 (2011). doi:10.1029/2010WR009144
Mao, D., Yeh, T.C.J., Wan, L., Wen, J.C., Lu, W., Lee, C.H., Hsu, K.C.: Joint interpretation of sequential pumping tests in unconfined aquifers. Water Resourc. Res. **49**, 1782–1796 (2013)
Mao, D., Yeh, T.C.J., Wan, L., Hsu, K.C., Lee, C.H., Wen, J.C.: Necessary conditions for inverse modeling of flow through variably saturated porous media. Adv. Water Resourc. **52**, 50–61 (2013)
McKenna, S., Poeter, E.: Field example of data fusion for site characterization. Water Resourc. Res. **31**(12), 3229–3240 (1995)
Mishra, P.K., Neuman, S.P.: Improved forward and inverse analyses of saturated-unsaturated flow toward a well in a compressible unconfined aquifer. Water Resourc. Res. **46**, W07508 (2010). doi:10.1029/2009WR008899
Mishra, P.K., Neuman, S.P.: Saturated-unsaturated flow to a well with storage in a compressible unconfined aquifer. Water Resourc. Res. **47**(5), W05553 (2011). doi:10.1029/2010WR010177

Moench, A., Garabedian, S., LeBlanc, D.: Estimation of Hydraulic Parameters from an Unconfined Aquifer Test Conducted in a Glacial Outwash Deposit, Cape Cod, Massachusetts. In: US Geological Survey Professional Paper, vol. 1629, pp. 1–51. US Geological Survey, Reston (2001)

Moench, A.F.: Importance of the vadose zone in analyses of unconfined aquifer tests. Ground Water **42**(2), 223–233 (2004). doi:10.1111/j.1745

Neuman, S.P.: Theory of flow in unconfined aquifers considering delayed response of the water table. Water Resourc. Res. **8**(4), 1031–1045 (1972)

Neuman, S.: Generalized scaling of permeabilities; validation and effect of support scale. Geophys. Res. Lett. **21**(5), 349–352 (1994)

Neuman, S.P., Blattstein, A., Riva, M., Tartakovsky, D.M., Guadagnini, A., Ptak, T.: Type curve interpretation of late-time pumping test data in randomly heterogeneous aquifers. Water Resourc. Res. **43**, W10421 (2007). doi:10.1029/2007WR005871

Oliver, D.S., Reynolds, A.C., Liu, N.: Inverse Theory for Petroleum Reservoir Characterization and History Matching, vol. 380, 1st edn. Cambridge Unviersity Press, Cambridge (2008)

Pan, L., Warrick, A.W., Wierenga, P.: Downward water flow through sloping layers in the vadose zone: time-dependence and effect of slope length. J. Hydrol. **199**, 36–52 (1997)

Portniaguine, O., Solomon, D.: Parmater estimation using groundwater age and head data, Cap Cod. Massachusetts. Water Resourc. Res. **34**(4), 637–645 (1998)

Reynolds, D.A., Marimuthu, S.: Deuterium composition and flow path analysis as additional calibration targets to calibrate groundwater flow simulation in a coastal wetlands system. Hydrogeol. J. **15**, 515–535 (2007)

Russo, D., Zaidel, J., Lauter, A.: Numerical analysis of flow and transport in a combined heterogeneous vadose zone-groundwater system. Adv. Water Resourc. **24**, 49–62 (2001)

Saiers, J.E., Genereux, D.P., Bolster, C.H.: Influence of calibration methodology on ground water flow predictions. Ground Water **42**(1), 32–44 (2004)

Sakaki, T., Frippiat, C.C., Komatsu, M., Illangasekare, T.H.: On the value of lithofacies data for improving groundwater flow model accuracy in a three-dimensional laboratory-scale synthetic aquifer. Water Resourc. Res. **45**, W11404 (2009). doi:10.1029/2008WR007229

Sanchez-Vila, X., Carrera, J., Girardi, J.: Scale effects in transmissivity. J. Hydrol. **183**, 1–22 (1996)

Scalon, B.R., Healy, R.W., Cook, P.G.: Choosing appropriate techniques for quantifying groundwater recharge. Hydrogeol. J. **10**, 18–37 (2002)

Schulze-Makuch, D., Carlson, D., Cherkauer, D., Malik, P.: Scale dependency of hydraulic conductivity in heterogeneous media. Ground Water **37**(6), 904–919 (1999)

Simmers, I.: Groundwater Recharge: An Overview Of Estimation "Problems" and Recent Developments, pp. 107–115. Geological Society of London, London (1998)

Tan, S., Shuy, E., Chua, L.: Regression method for estimating rainfall recharge at unconfined sandy aquifers with an equatorial climate. Hydrogeol. Process. **21**, 3514–3526 (2007)

The Mathworks Inc.: Optimization Toolbox^{TM} Users Guide. Mathworks, Natick (2012)

Tiedeman, C.R., Hill, M.C., D'Agnese, F.A., Faunt, C.C.: Methods for using groundwater model predictions to guide hydrogeologic data collection, with application to the Death Valley regional groundwater flow system. Water Resourc. Res. **39**(1), 1010 (2003). doi:10.1029/2001WR001255

Wang, D., Zhang, Y., Irsa, J.: Proceeding of the 2013 AGU Hydrology Days (2013). http://hydrologydays.colostate.edu/Papers_13/Dongdong_paper.pdf. Accessed 16 August 2013

Zhang, Y., Gable, C.W., Person, M.: Equivalent hydraulic conductivity of an experimental stratigraphy–implications for basin-scale flow simulations. Water Resourc. Res. **42**(7), W05404 (2006). doi:10.1029/2005WR004720

Zlotnik, V.A., Zurbuchen, B.R.: Estimation of hydraulic conductivity from borehole flowmeter tests considering head losses. J. Hydrol. **281**, 115–128 (2003)